AIRBUS

CARGO DRONE

CHALLENGE

PRESENTED BY

LOCAL MOTORS

IN PARTNERSHIP WITH

AIRBUS

GROUP

AUTHORS:

Cuerno-Rejado, Cristina; Sánchez-Carmona, Alejandro; García-Hernández, Luis; Fernández-López, Antonio; Sánchez-Guillén, Francisco José; Álvarez-Llorián, Paula; Gómez-Rodríguez, Álvaro; Sopo-López, Ángel; Rodrigo-Pascual, Pablo; Cabeza-Moreno, Francisco Javier; Rodríguez-Alonso, Diego; Villanueva-Cañizares, Carmelo Javier; Robles-González, Víctor; Baldereschi-de-Cascante, Diego.

ABOUT THE AUTHORS

All authors are members of the Technical University of Madrid and their profiles are quite different:

Cuerno-Rejado, Cristina is **Full Professor** of this University in the Aircraft and Spacecraft Department, specialised in Conceptual and Preliminary design.

Sánchez-Carmona Alejandro and *García-Hernández, Luis* are **PhD students** whose PhD Thesis are about "Study of unconventional tail configurations for commercial transport airplanes" and "Study of robust fault-tolerant autopilots" respectively. Both are working in the Aircraft and Spacecraft Department too. Furthermore, *Sánchez-Carmona, Alejandro* is **Lecturer** of the same Department.

Fernández-López, Antonio is also **Associate Professor** at the University, expert on composites and with great experience in this field due to his job at Airbus for many years.

Sánchez-Guillén, Francisco José is an **Aeronautical Engineer** from the same University.

Álvarez-Llorián, Paula and *Baldereschi-de-Cascante Diego* are **Master in Aeronautical Engineering Students**.

Gómez-Rodríguez, Álvaro; Sopo-López, Ángel; Rodrigo-Pascual, Pablo; Cabeza-Moreno, Francisco Javier; Rodríguez-Alonso, Diego; Villanueva-Cañizares, Carmelo Javier and *Robles-González, Víctor* are **Bachelor Degree in Aerospace Engineering Students**. Each one is working on their own Final Thesis.

INDEX

INDEX OF FIGURES

INDEX OF TABLES

1. BRIEF DESCRIPTION

The idea of this design is to combine the advantages of fixed and rotary wing aircraft. Rotary wing aircraft can perform vertical take-off and landing, hover flights and also can operate in more difficult localizations. However, horizontal flight performance of these type of RPAS are less efficient because the energy consumption is higher and also the flight speed is lower. In order to improve these two aspects, the hybrid solution between fixed and rotary wing is achieved. Fixed wing aircraft are more efficient from the standpoint of cruise flight. Thus, take-off and landing phases of the flight are carried out as rotary wing and cruise flight as fixed wing aircraft. The change between the two modes of functioning is done by reducing the power transmitted to the vertical rotors at the same time that it is transmitted to the tail rotor to increase horizontal speed. Once enough speed is reached, the fixed wings can lift the whole weight of the RPA, the vertical rotors are turned off and left at minimum drag position. In spite of that, a slight penalization is paid in terms of drag for cruise flight. Furthermore, the aircraft can take-off and land as fixed wing aircraft if it is necessary.

The materials used for manufacturing are composites. The techniques used for these materials are simpler than those used on commercial aviation, in order to reduce manufacturing costs. In addition, the performance of these materials is better than that of those typically used on models or toys. Finally, these aircraft can be used for trying new technologies like sensors embedded in the structure in order to track the deformations and predict premature element failure.

The performances developed by this RPA depend on the configuration selected. The manufacturing is centered on modularity, so the wings and tail cone can be demounted for easing transportation and also allow changing the tail motor and propeller. The combination of tail motor and propeller can be chosen to maximize endurance, range or cruise speed, depending on the mission of the aircraft. This feature gives the RPA a great versatility. Thus, the maximum endurance of the aircraft is 130 min, without payload. Another advantage is that the maximum endurance configuration is also the maximum range one. This maximum range is 170 km. On the other hand, the maximum speed reached depends on the powerplant. In spite of that, maximum speed is limited at 190 km/h electronically. Note that the higher the cruise speed, the lower the range and endurance.

In view of these performances, the missions that can be carried out by this RPA are very diverse. For example: crop monitoring, monitoring of pollution, inspection of power-lines and fire prevention.

The final dimensions of the RPA have been reached following the procedure presented in Figure 1-1. This procedure presents three iteration loops: weight loop, aerodynamic loop and performances loop. The convergence of weight and aerodynamic loops have been reached simultaneously. Once this has been done, the performance loop is executed and converged.

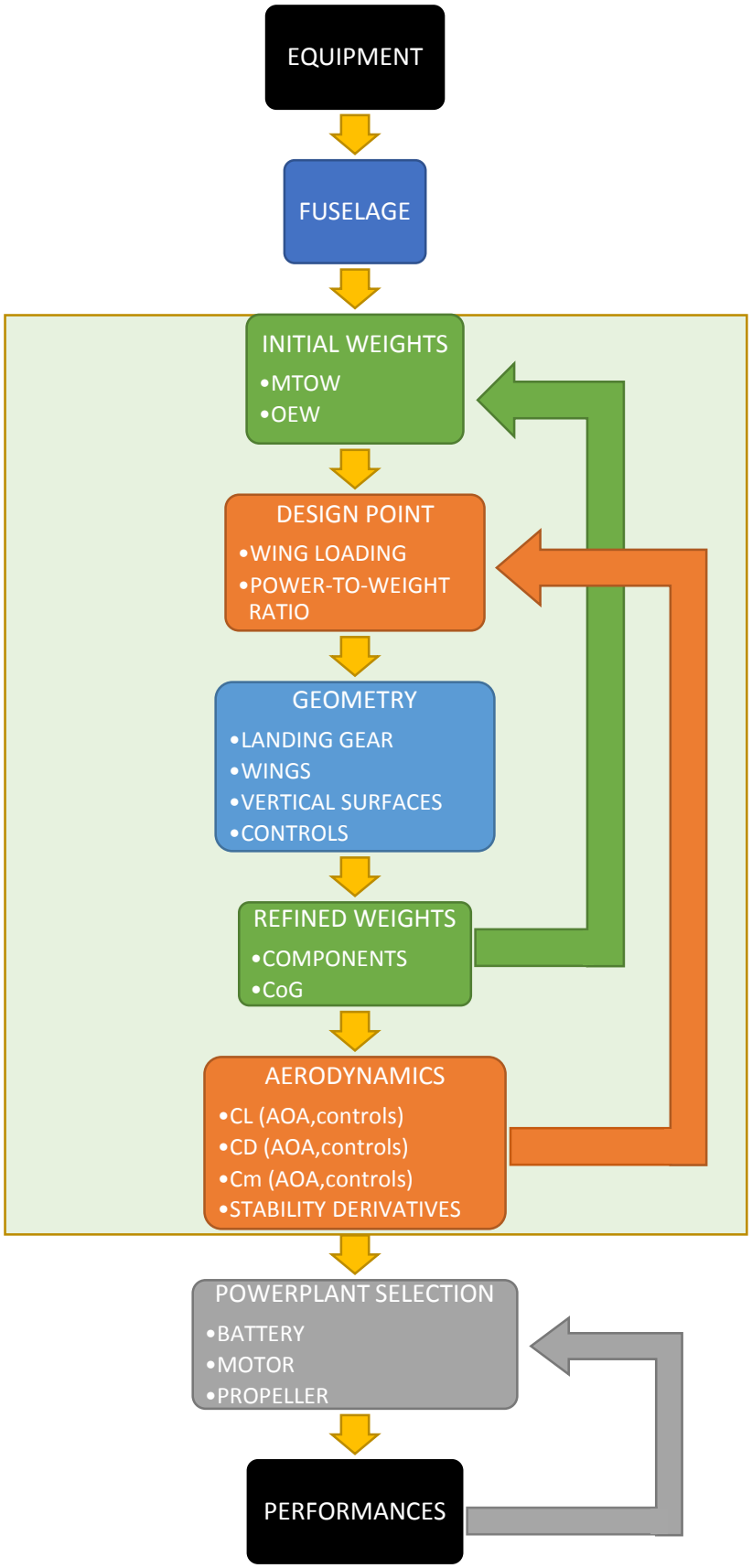

Figure 1-1 Iterative design procedure.

2. DETAILED DESCRIPTION

2.1. STRUCTURAL CONCEPT

2.1.1. Fuselage

The fuselage is divided into three parts: front, central and rear. The front part is a semi-ellipsoid, where avionics systems and the camera are located. The central part is a rectangular prism with rounded corners section. This part is in charge of housing the payload, the batteries, the IMU and the parachute system. The rear part has rectangular pyramidal form with rounded corners section. This part is responsible for housing the rear powerplant and the attachments for rear wing and for vertical stabilizers.

The dimensions of the fuselage have been obtained imposing some constraints. The first one is transportability: total length of the fuselage cannot exceed 2 meters. Then, the relation between the three parts of the fuselage has been established in 25%, 50%, and 25% of the total length. Analyzing Table 2-1, where all equipment dimensions are included, the width and the height of the prismatic part can be determined by increasing in a certain factor the volume occupied by that equipment. The final dimensions of the fuselage are included in Table 2-2.

From the standpoint of the structural concept, the fuselage consists of a beam that bears the loads transmitted by the wings and is also responsible for supporting the equipment. In addition, this equipment is supported by frames, which bear no structural loads. The external geometry is defined by a light skin. The materials used for manufacturing are included in Section 2.2.

	Length [mm]	Width [mm]	Height [mm]
Flight Control Computer	170	180	80
Internal Measurement Unit (IMU)	100	30	40
ADS-B Transponder	89	46	18
Antennas and external mounted Systems	-/-	-/-	-/-
Flight Termination Parachute	280	120	50
Flight Termination System/Launcher	200	55	55
Camera System	97	95	97
Communication System	57	98	86
Payload	472.5	367.5	210
Induction System Charger	173.5	93.2	43.2
Induction System Coil	300	300	10

Table 2-1 Equipment list dimensions.

	Units	Value
Length	m	1.99
“Cylindrical zone” length	m	0.99
Nose length	m	0.50
Rear end length	m	0.50
Max Width	m	0.42
Max Height	m	0.33
End Width	m	0.1
End Height	m	0.1

Table 2-2 Fuselage geometry.

2.1.2. Wings

The procedure for obtaining the final wings geometry is divided into three steps: analysis of the design point, definition of the geometry by non-dimensional variables and aerodynamic analysis. The analysis of the design point is based on the relation between the power-to-weight ratio and the wing loading. Several conditions impose restrictions to this relation. The conditions considered in this project are: cruise flight at constant speed, climb at constant speed and climb angle, and gusts conditions for cruise speed and maximum horizontal speed. The two first conditions impose a minimum value to the power-to-weight ratio for each wing loading. On the other hand, gusts conditions impose a minimum value to the wing loading, independently of the power-to-weight ratio. Because an initial estimation of the weight can be carried out (further explanations in section 2.6), once the design point is selected, the wing area and the power of the motor are also fixed. In the second step, the wing planforms are designed through non-dimensional variables in order to reach the wing area obtained previously. These non-dimensional variables are marked in cursive and bold font in Table 2-3. From these ones, the rest of variables can be determined. Table 2-3 includes the final result of wing geometries. The final step is the aerodynamic analysis. The main idea is to design the wings so that with zero angle of attack the aircraft lifts enough for cruise flight and is also balanced without deflection of control surfaces for cruise flight. The result of this analysis is the value of the incidence angles of the two wings. The airfoil selected for the two wings and the values of the incidence angles are also included in Table 2-3.

From the standpoint of inner structure, it has been decided to use a classical solution which is a structure based on ribs and stiffeners. Further explanations about this structure in section 2.2.

	Units	Value
Wing area	m^2	0.626
Aspect ratio	-	***8.0***
Span	m	2.237
Taper ratio	-	***0.66***
Root chord	m	0.337
Tip chord	m	0.222
Leading edge sweep	º	2.9
Dihedral angle	º	***0.0***
Longitudinal position	m	***0.717 / 1.514***
Airfoil	-	CLARK-Y-B
Incidence angle	º	1.24 / -0.53

Table 2-3 Wings geometry. Where a slash appears, the left value corresponds to front wing and the right value to rear wing.

2.1.3. Landing gear

A classical landing gear in a tricycle configuration is proposed. However, no correlation provided by similar aircraft can be used because some resultant parameters do not assure safe taxi or landing operations.

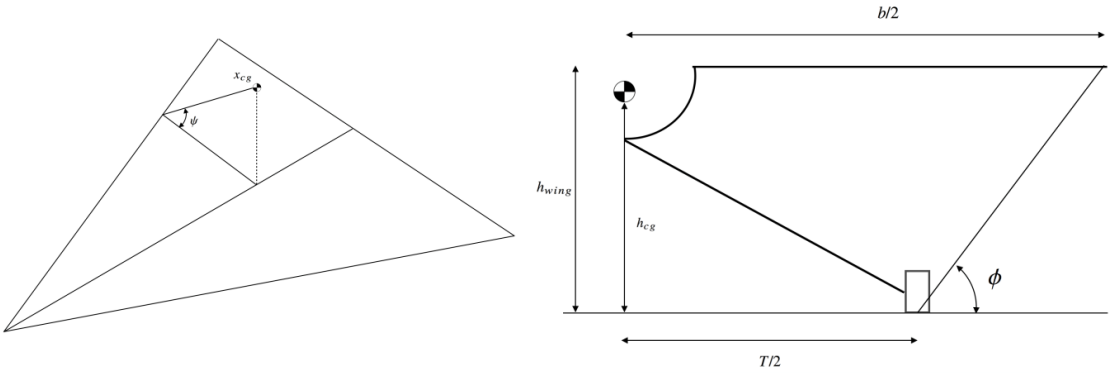

Figure 2-1 ψ angle defined by track, wheelbase and h_{cg} (left) and ϕ angle defined by track, wingspan and h_{wing} (right).

	Value	Restriction
Xnose(m)	0,35	>0,3
Xmain(m)	1,45	>1,4
Track(m)	1,3	-
Wheelbase(m)	1,1	-
lm(m)	0,45	-
Xcg(m)	1	≈1
h_{cg}(m)	0,414	>0,4
b(m)	2,211	2,211
h_{wing}(m)	0,4604	0,4604
ϕ(º)	45,31	>8
ψ(º)	47,15	<55

Table 2-4 Restrictions and Values.

Once the length of the landing gear bars have been calculated, having the partlist of the different needed components and using the different densities of the materials, the total mass value can be estimated in:

$$M_{main\ LG} = 0.596\ kg$$

$$M_{nose\ LG} = 0.143\ kg$$

The dimensions of the bars are:

	Quantity	Mass (kg)	Total Mass (kg)	Main Lengh (mm)	t (mm)
Nose Bar	1	0,053	0,053	250	10
Left Bar	1	0,25	0,25	696	13
Right Bar	1	0,25	0,25	696	13

Table 2-5 Dimensions of the landing gear bars.

2.1.4. Waterproofness

The waterproofness requirement is satisfied by sealing all the modular elements with each other, since the materials used are waterproof. In addition, the manufacturer of the equipped batteries ensures that they are waterproof (Else (CEO), 2016).

2.1.5. 3-view drawing

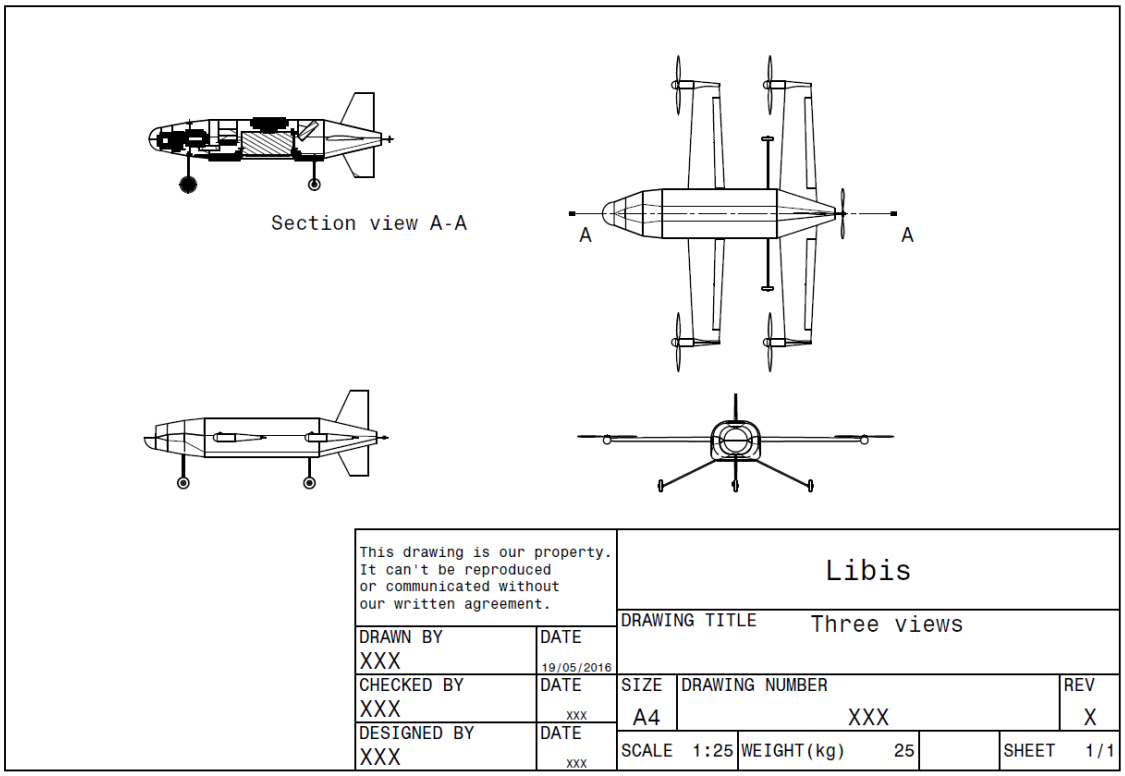

Figure 2-2 Three views.

2.2. MATERIALS AND MANUFACTURING

The manufacturing of the LIBIS composite structure should deal with different issues:

- To **minimize production costs/time** for the manufacturing of parts: Out of Autoclave materials allows to use.
- To seek a **high level of integration** of parts to improve surface quality.
- **Modular assembly to fuselage.**
- To develop a structure capable of realizing **Natural Laminar Flow (NLF)** on the upper and lower side: surface quality which meets NLF requirements regarding steps, gaps, 3D disturbances, waviness.

In order to obtain the best structural performances, different technologies have been selected to provide a high quality manufacturing process. As most of the properties of the final part have a high dependency with the tooling quality, it has been developed a specific process to manufacture composite tooling.

For this process, the **Additive Layered Manufacturing (ALM)** has been selected in order to obtain a **Master Model**. In a first step, a rough geometry has been obtained by

Fused Deposition Modeling (FDM) of ABS. This first model will provide **high dimensional accuracy**, but low surface quality. The geometry obtained from the 3D printer present gaps between the fused ABS strips. The gaps will be fulfilled with epoxy resin for tooling (Laminating Tooling Resin (ET-05)) in order to produce a hard, durable surface coat at the curing temperature (180ºC). Next, a final mechanizing could be promoted in order to obtain a **high surface quality.**

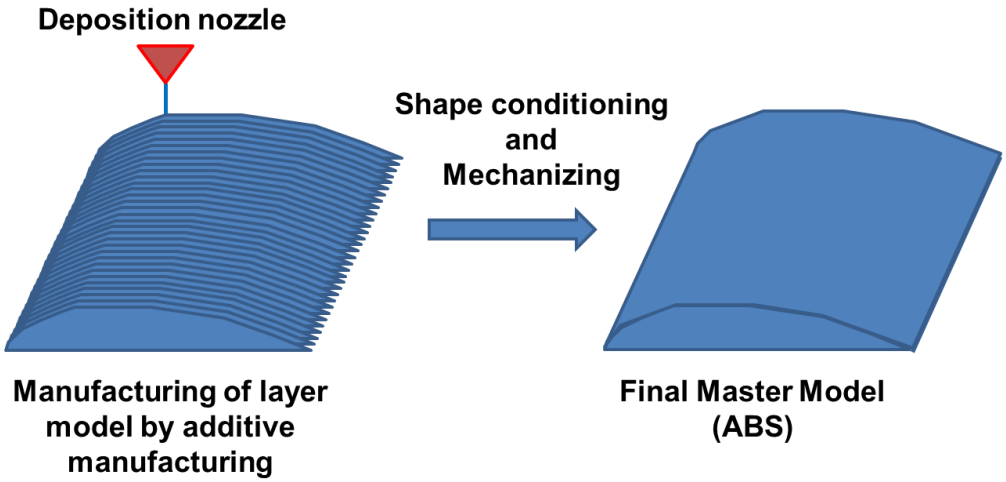

Figure 2-3 Scheme of Master Model manufacturing.

Figure 2-4 Picture of the master model manufactured by ALM.

With the surface optimized version of the Master Model it will be manufactured a **composite tool by laminating HEXTOOL** over the master. HEXTOOL is a composite prepreg specially designed for molding manufacturing, and it will allows laminating and curing composite materials up to 180 º C. ABS allows to pre-cure the HEXTOOL at 120ºC. Then, a postcuring process at 180ºC will be necessary. As the manufacturing process maintains the dimensional stability, tolerances are similar to those achieved with metal tooling. Vacuum integrity is assured, even in heavily machined areas.

By this procedure it is possible to manufacture **high quality composite tooling by a cheaper, customized and robust procedure**.

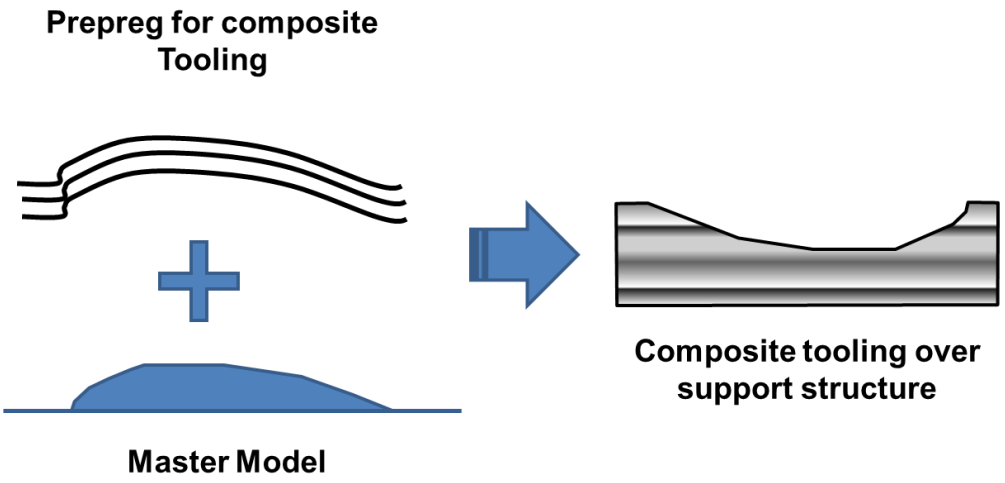

Figure 2-5 Scheme of manufacturing of composite tooling of aerodynamic surfaces.

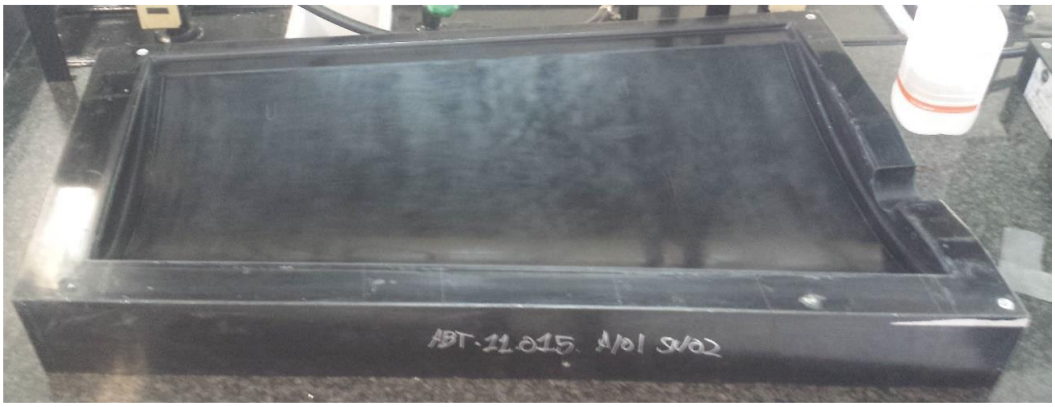

Figure 2-6 Picture of composite tooling of aerodynamic surfaces.

Afterwards, the tooling surface could be used for lay-up and curing. For LIBIS structure, a **co-bonding** process has been selected in order to obtain a **high integration**. **Stiffeners and ribs are pre-cured, and then mounted over the skin without curing**. The wing structure will be closed by a secondary bonding. The material chosen is an **Out of Autoclave (OoA) prepreg M56**, which allows obtaining a composite material with low porosity and high fiber content only assisted by vacuum. This material will require only a vacuum bag and an oven, reducing extremely the manufacturing cost. Once the structure is finished and mounted, a surface veil is applied to improve the surface quality and allows realizing **Natural Laminar Flow (NLF)**.

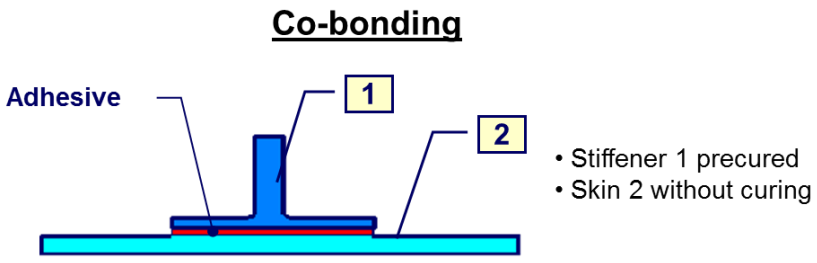

Figure 2-7 Scheme of co-bonding process for stiffener integration on skin.

Figure 2-8 Picture of the integrated structure.

Figure 2-9 Picture of a vacuum bag on composite tooling.

The **modular assembly** is performed by **fixing two metallic parts** on the rib closer to the fuselage. These modules will be mounted on the cured rib, and will allow an easy assembly to the fuselage.

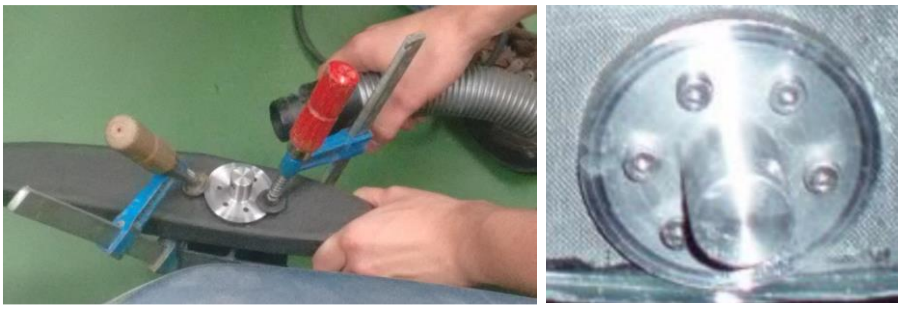

Figure 2-10 Integration of the metallic assembly fixture on composite rib.

2.3. INDUCTION SYSTEM

The fundamental characteristic of induction charging is that it does not require direct contact between metals, which results in the following advantages:

- **More durable charging**: There are no electrodes that can be corroded by the action of weather.
- **Better modularity, easier maintenance:** The coils and internal circuits can be easily replaced without affecting the structure.
- **Safer charging**: There are no metal pieces in contact.

- **Remote operation**: No direct human intervention.
- **Wider scope of missions**: The system not only allows to operate the RPA in a wider range of weather conditions, but also increases the range by placing several charging pads.

2.3.1. DESCRIPTION OF THE SYSTEM

The system relies on the principle of transmitting energy through magnetic fields.

It consists in two electromagnetically coupled coils to transmit the energy onto the RPA. A first coil is placed inside the charging station and is responsible for transforming the power from the power supply into an oscillating electromagnetic field. A second coil sits inside the RPA, and converts this oscillating electromagnetic field back to electricity. This alternate current cannot be directly fed into the batteries, so additional circuits must be included in order to transform, rectify and filter this input.

2.3.2. RESULTS

In order to analyse the feasibility of the induction system, an approximation to the real circuit was developed. For a more detailed analysis, turn to reference (Angrisani, 2015). Calculations have shown that the efficiency of this process is highly dependent on the relative distance of the coils, the closer they are the less energy is lost. For this reason, a mechanism that rises and brings both coils together has been devised (Section 3.6). Another important factor is the operating frequency of the system. High frequencies have proven to be beneficial to the performance.

The design configuration sets the induced coil, placed inside the RPA, to be 100g in mass and 30cm in diameter placed in front of the payload compartment. To avoid electromagnetic interference, this coil can be placed inside an insulating cage.

The inductive coil is similar in size, and the distance between the two is 5 cm. With these parameters, an estimated performance of 70% has been obtained. The charging time could be optimised to fulfil the requirements of the particular mission, but calculations lead to an estimated time of 60 minutes.

2.4. PAYLOAD SYSTEM

2.4.1. Payload anchoring system

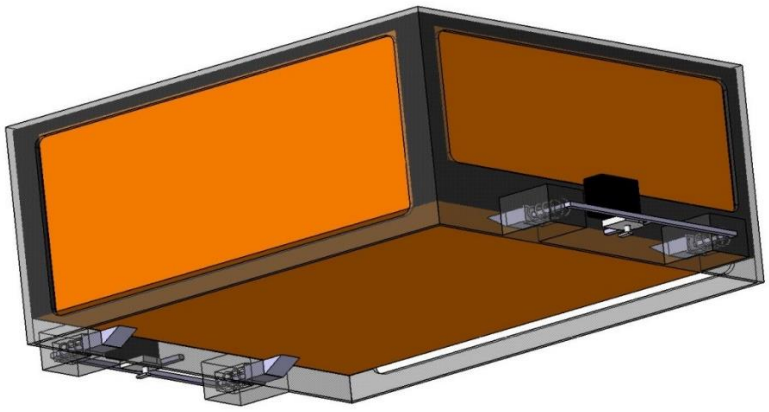

Figure 2-11 Payload System 3D view.

As shown in Figure 2-12, the payload anchoring system consists of four latches (1) that block the payload (2), four springs (3) that block the latches, two servos (4) and two bars (5) that move the latches and let the payload free. Fuselage structure (6) has been modified in order to contain the payload. A slim rubber layer (7) has been added between this structure and the payload in order to soften the payload movement in the fuselage and during anchoring or releasing operations.

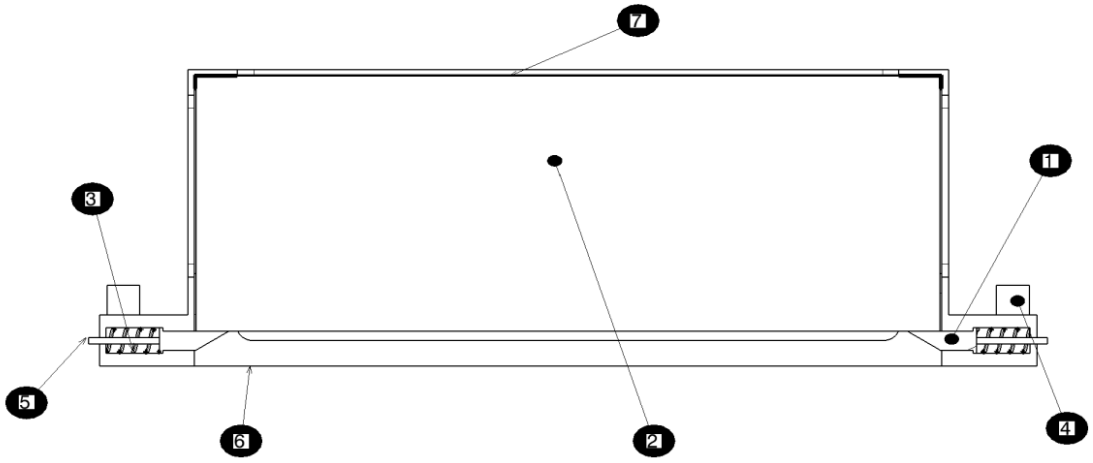

Figure 2-12 Payload System 2D view.

Before trying to load the payload into the aircraft, the bars are free but the springs block the latches. The shape in which the latches have been produced lets them move horizontally when a vertical force is applied. This force is applied by the payload. Once the latches have been moved, the payload can get into the fuselage. When it reaches the top, the springs pull the latches and block the payload. When proceeding to free it, servos pull back the latches and the payload is released.

- **Latch**: 40x20x15 mm, 25g each, Aluminium. It blocks the payload.
- **Spring**: D20x32 mm, 10g each, SF-TF-1524-SS1774-04-Lesjofors. It blocks the latches.
- **Servo**: HS-645MG, 55g each. It moves the bar which moves the latches and lets the payload free.
- **Bar**: 20g each, Aluminium. It connects the servo with the latches.
- **Rubber layer**: It softens the payload movement in the fuselage and during anchoring and releasing operations.

The whole system weight is 290 g and it has been designed in order to allow it to deliver the payload to the landing platform or release it during the flight.

2.4.2. Doors system

As shown in Figure 2-13, the gates system consists of two servos, two bars and two doors. The servo pulls down the bar which in turn pulls down the doors. Each bar has a mechanism which allows it to adapt its shape to the movement of the doors. The servos used are HS-645MG. The total weight of the system is 110 g.

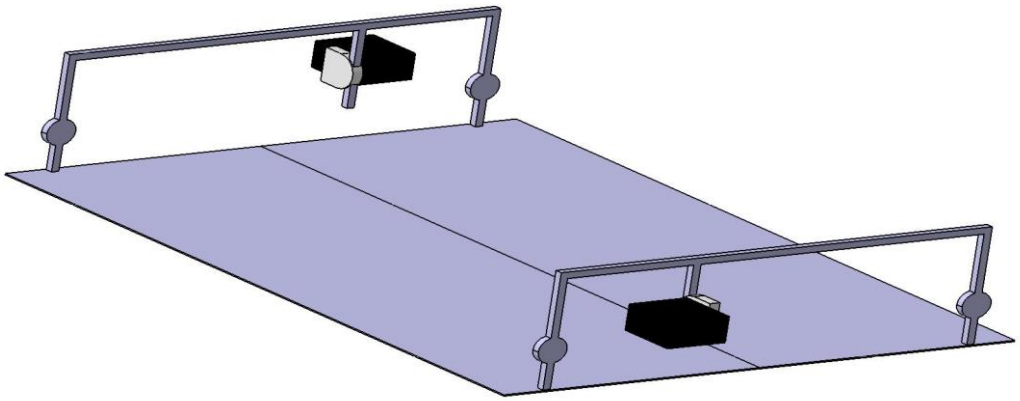

Figure 2-13 System of the doors.

2.4.3. Operation in case of failure

If the payload release system is not operative for any reason, one can switch off all servos and move the bars manually with two cranks. This system is accessible from the lower side of the fuselage. The weight of the payload opens the doors and it is released.

2.5. PARACHUTE SYSTEM

The parachute recovery system allows the vehicle to reduce the impact speed in case of a failure that compromises the safety of the flight, preventing major damages on the ground.

The parachute system proposed is the Skycat XL-96, a system based on a pilot and a main chute which helps to extract the second one. The main characteristics of the system and launcher are shown below:

- Main chute: Iris Ultra 96, annular; Deployed Ø: 2.44 m; Cd: 2.2; Total weight w/container and lines: 0.77 kg.
- Pilot chute: Iris Ultra 48, annular; Deployed Ø: 1.22 m; Cd: 2.2; Total weight: 0.12 kg.
- Launcher: Skycat X55-CF; Total weight: 0.157 kg.

The total weight of the system is 1.047 kg, plus an estimated installation weight of 15%.

The main chute is packed and attached to the frames of the mid-section of the fuselage, over the CG and under the slotted skin, with an easy-removable cover. The launcher is inserted in the same way behind it, in a 45^0 angle to allow a correct deployment of the pilot chute (packed in the launcher).

The terminal speed during steady descent with the parachute deployed would be approximately 6.9 m/s. ASL. If two main chutes are used, the terminal speed would be reduced to 4.4 m/s, but the weight of the system could increase over 80%. A better way to reduce the terminal speed (the manufacturer of the IFC-96 recommends a maximum vehicle weight of 23 kg) is to increment the deployed area of the main chute. This would only increase the material weight of the chute and the lines, but the launcher and the harness lines could remain the same, as the deployment force stands low for low speeds.

The forces and terminal speeds depend on the type of chute used. Some common types are shown in Table 2-6:

Type	Opening force factor	Drag coefficient
Circular/annular (solid)	High	High
Cross-shaped (solid)	Medium	Medium-high
Circular slotted	Medium-low	Low

Table 2-6 Main chute types performance.

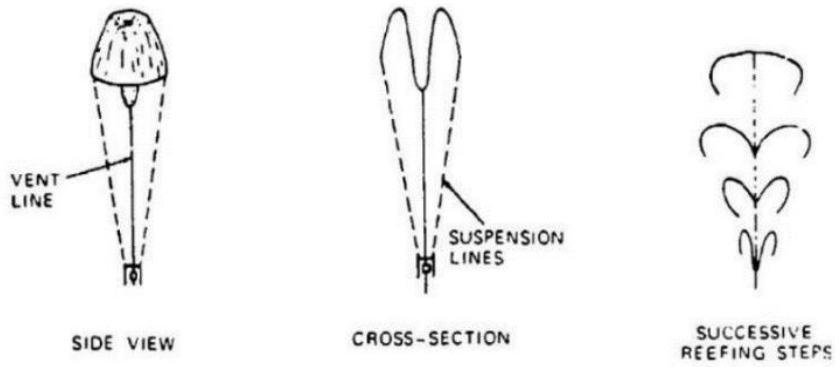

Figure 2-14 Vent reefing (Knacke, 1991).

There are methods to reduce the opening force on a circular chute, which would allow to increase the maximum opening speed. The *reefing* method consists on controlling the filling process of the canopy, staggering it and reducing the opening shock. The reefing method shown above could be used in the IFC-96 controlling the length of the center line attached to the apex.

2.6. TABLE OF WEIGHTS

The determination of the weight of the aircraft is divided into two steps. In the first step, general values of the weights are obtained, and in the second step refined values of weight are determined, which must be compatible with the weights of the first step. Table 2-7 shows the values of the general weights. These values are calculated through classical correlations imposing the weight of all equipment (Table 2-8) carried by the aircraft. This estimation of the MTOW is used in the analysis of the design point in order to determine the wing area and the power of the rear motor.

	kg
MTOW	24.990
OEW	16.180
Structure Weight	10.821
Avionics & Systems Weight	4.428
Installations Weight	0.931

Table 2-7 Main weights.

	Weight [kg]	x CoG [m]
Flight Control Computer	0.500	0.384
Internal Measurement Unit	0.050	1.036
ADS-B Transponder	0.100	0.244
Antennas and external mounted Systems	0.280	0.173
Flight Termination Parachute	0.890	1.036
Flight Termination System/Launcher	0.157	1.385
Camera System	0.420	0.128
Communication System	0.500	0.228
Induction System: Charger	0.300	0.505
Induction System: Coil	0.100	0.568
Payload System	0.400	1.036
Wiring and installations	0.931	-

Table 2-8 Equipment weights and CoG location.

Refined calculations estimate the weight of each component of the structure. These calculations are based on classical correlations properly modified in order to collect the distinctive features of this design. For example, the manufacturing techniques or the materials. In fact, wing prototypes are being manufactured and this has highlighted the validation of the weights obtained. The results of this refined study are included in Table 2-9. In addition, other weights which have to be taken into account correspond to the propulsion system. This system is formed by motors, controllers, propellers and batteries. Depending on the performances of the mission, these components change. Table 2-10 includes the weights of this system for each of the proposed missions.

	Weight [kg]	x CoG [m]
Fuselage	2.979	1.096
Front Wing	0.908	0.857
Rear Wing	0.908	1.612
Upper Vertical Fin	0.372	1.678
Down Vertical Fin	0.233	1.677
Front Control Surfaces (with actuators)	0.952	0.934
Rear Control Surfaces (with actuators)	0.786	1.731
Landing Gear	0.787	1.377

Table 2-9 Structural weights and CoG location.

	Range=60 km, MTOW		Range=100 km, MTOW	
	Weight [kg]	x CoG [m]	Weight [kg]	x CoG [m]
Rear End Motor (REM)	0.515	1.954	0.515	1.954
Controller REM	0.055		0.055	
Propeller for REM	0.132		0.132	
Rear VTOL Motors (RVM) x2	1.030	1.571	1.030	1.571
Controllers for RVM x2	0.110		0.110	
Propellers for RVM x2	0.336		0.336	
Front VTOL Motors (FVM) x2	1.030	0.784	1.030	0.784
Controllers for FVM x2	0.110		0.110	
Propellers for FVM x2	0.336		0.336	
Battery 1	1.690	0.700	3.380	0.550
Battery 2	1.690	0.700	1.690	1.370
Equipment Battery	0.430	0.600	0.628	0.600
Payload	5.05	1.036	3.16	0.967

Table 2-10 Propulsion system and Payload weights and CoG location.

The Operating Empty Weight (OEW) includes the structure and all the equipment necessary for flight without batteries. Thus, the addition of the weights of the structural

components and propulsion system is equal to the OEW estimation in the first step. The weight distribution of the OEW is indicated in Figure 2-15. The weight distribution for each proposed mission has been included in Figure 2-16.

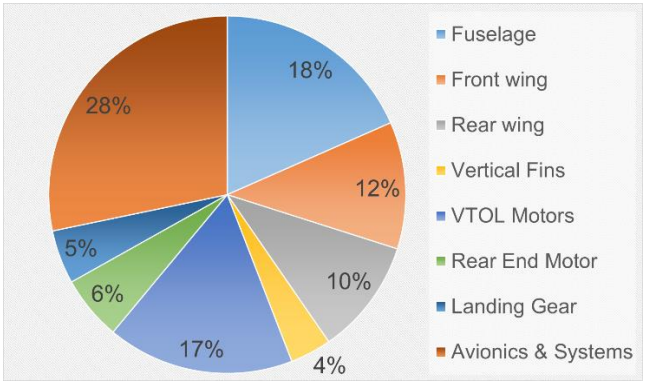

Figure 2-15 Weights distributions for Operating Empty Weight.

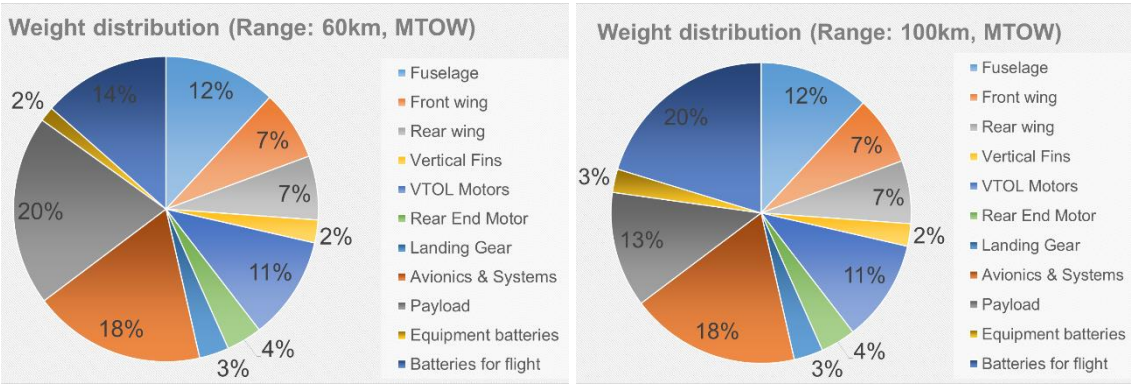

Figure 2-16 Weights distributions for design missions.

2.7. EQUIPMENT LOCATION

The centres of gravity of all equipment and structure components are included in Table 2-8, Table 2-9 and Table 2-10. Of all the equipment, only the batteries are thought to be placed in different locations to ensure a desired static margin. The physical boundaries are presented in Table 2-11. Here it is possible to see that there are three locations for the batteries, two ahead of the payload and the other one on the back. In spite of these locations, it is not necessary that both are fulfilled. Because the equipment battery is smaller, the third interval of the Table is reserved for it. This location is close to the equipment in order to reduce the weight of the cables.

	x_{min} [m]	x_{max} [m]
Battery 1	0.548	0.721
Battery 2	1.373	1.670
Equipment Battery	0.299	0.721

Table 2-11 Geometrical boundaries of CoG positions for each battery station.

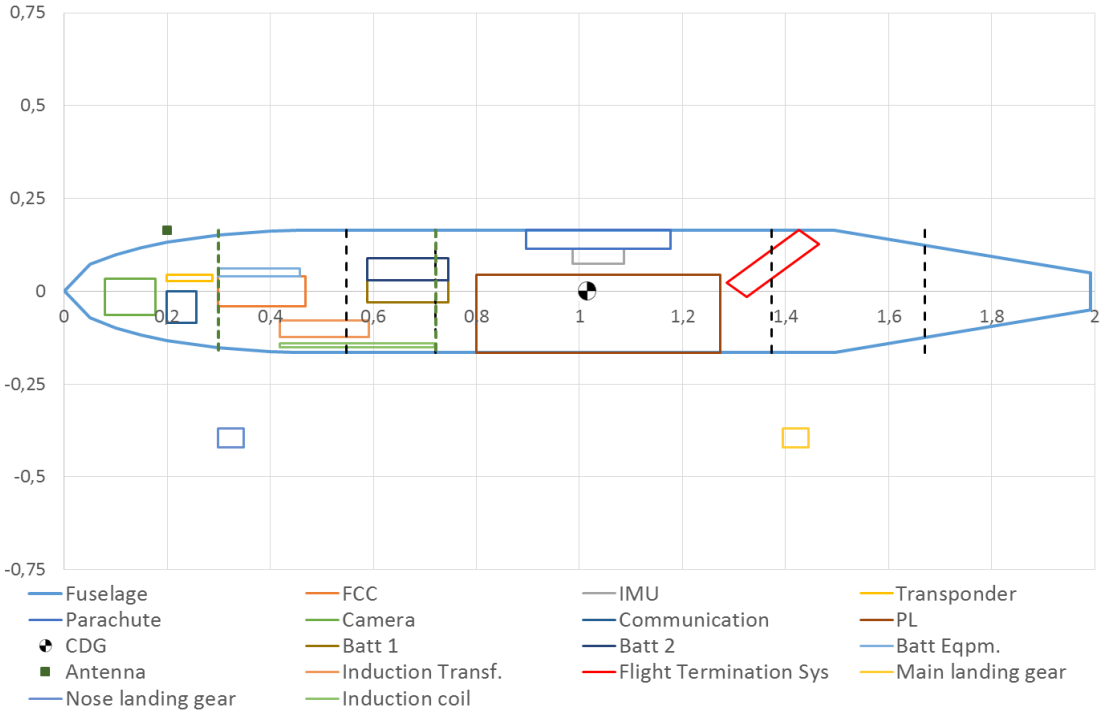

Figure 2-17 Scheme of equipment locations.

Table 2-12 shows the position of the centre of gravity in meters from the nose of the aircraft for both proposed missions and the static margin achieved in percentage of the mean aerodynamic chord.

	Range=60 km, MTOW	Range=100 km, MTOW
X_{CoG} [m]	1.015	1.013
Static Margin [%MAC]	25.45	25.9

Table 2-12 CoG position and Static Margin for design missions.

2.8. ISOMETRIC VIEW

Figure 2-18 Isometric view of the aircraft.

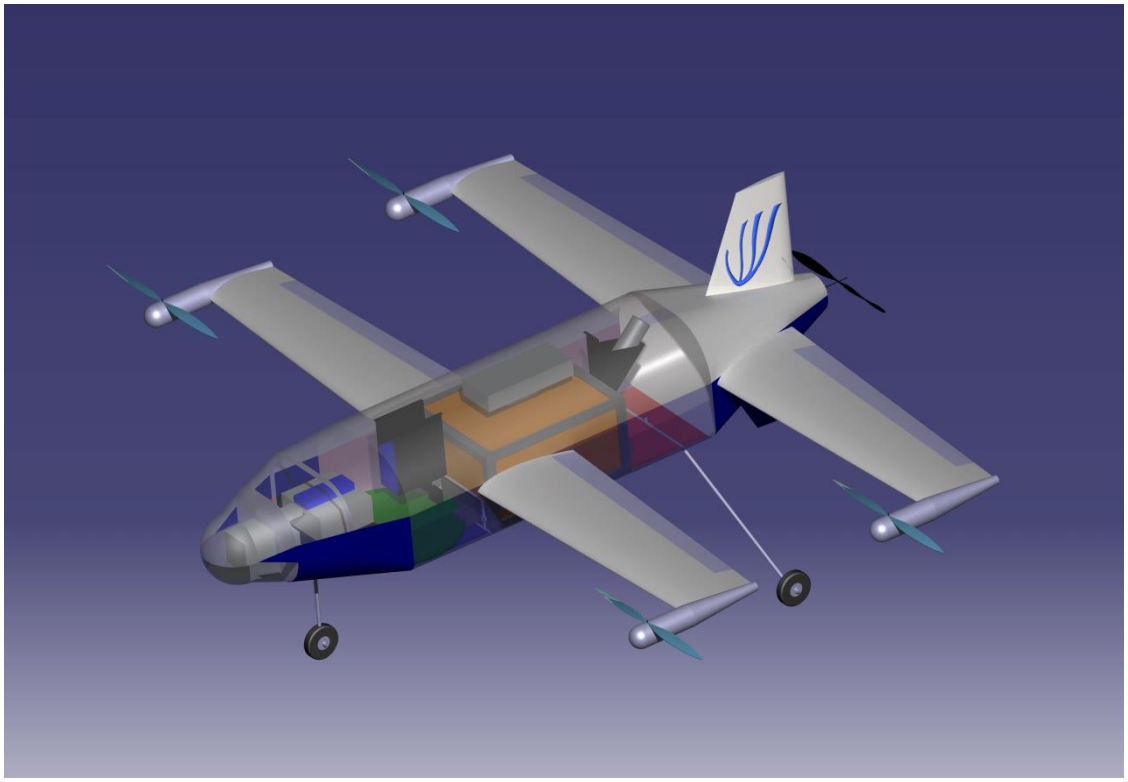

Figure 2-19 Isometric view of the equipment on-board the aircraft.

3. OPERATIONAL DESCRIPTION

3.1. DESIGN MISSION

The design missions proposed by the challenge are carried out as follows:

- Take-off: As rotary wing, from the ground to 300 feet with full throttle on VTOL motors.
- Acceleration stage: This stage is divided into two sub-stages. First, the weight of the aircraft is lifted by the rotary wing while the rear motor is giving horizontal speed to the aircraft. During this stage, the angle of attack is kept at minimum drag position. This stage ends when horizontal speed reaches stall speed. From this point, the power transmitted to VTOL motors is reduced linearly until cruise speed is reached, when VTOL are fully turned-off. In this second stage, the angle of attack changes in order to ensure enough lift force. At the end of this stage, the lift is generated only by the fixed wings. The estimation of the duration and energy consumption of this phase is carried out with a Runge-Kutta method integration. The horizontal distance travelled in this stage has been taken into account.
- Cruise flight: At maximum range speed (for the model used see Section 3.2).
- Loiter: during 5 minutes at maximum endurance speed. Because maximum endurance speed and maximum range speed are so close to each other, it has been decided to fly at the same speed in both stages.
- Descent stage: At 5º of descent angle. The constant speed reached in this stage is 32.1 m/s. The descent ends when a height of 33 feet is reached.
- Deceleration stage: From 32.1 m/s to 0 m/s. The hypothesis of this stage are similar to those of the acceleration stage.
- Landing: As rotary wing, from 33 feet to the ground.

A schema of the mission and the time and consumption analysis are included in Figure 3-1 and Table 3-1, respectively.

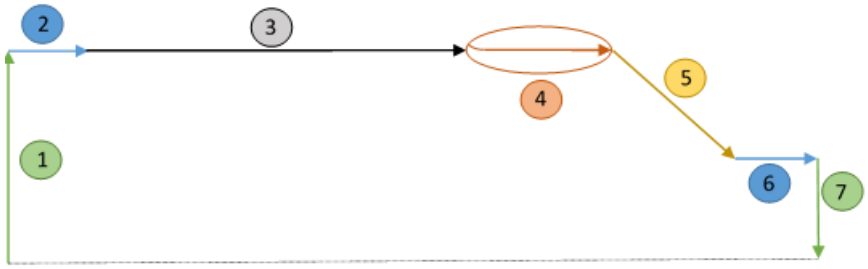

Figure 3-1 Flight profile.

	Phase	Duration [min]	Energy consumption [Wh]	Horizontal speed [m/s]	Vertical speed [m/s]	Height over ground [ft]
1	Take-off	0.76	54.32	0	2.5	0 – 300
2	Acceleration phase	0.13	9.86	0 – 23.11	0	300
3	Cruise flight	45.6 / 73.2	489 / 798	23.11	0	300
4	Loiter	5	37.25	23.11	0	300
5	Decent phase	0.48	1.76	31.98	-2.80	300 – 33
6	Deceleration phase	0.19	7.12	32.1 – 0	0	33
7	Landing	0.08	5.89	0	-2	33 – 0

Table 3-1 Time analysis of the design missions. In the case a slash appears in the cell, the left value applies for 5kg of PL and the right one for 3kg. In the case a hyphen appears in the cell, it indicates the variation interval of the magnitude.

3.2. OTHER PERFORMANCES

The modularity of the design allows to change the propulsion system depending on the required mission. Changes in propulsion system imply changes in cruise speed, climb rate and consequently the aerodynamic efficiency is also different (examples of these changes are included in Table 3-2). In addition, for each configuration of propulsion system, it is possible to interchange weight between payload and batteries until reaching MTOW. Since there are plenty of possibilities, here are shown only variations of the selected configuration for the design mission. Figure 3-2 illustrates payload-range and payload-endurance diagrams. These curves are theoretical, since equipment battery does not change while endurance increases. In practice, the higher the endurance the bigger the equipment battery needs to be. These diagrams include the same schema than Figure 3-1, where the only change is the consumption and duration of cruise stage.

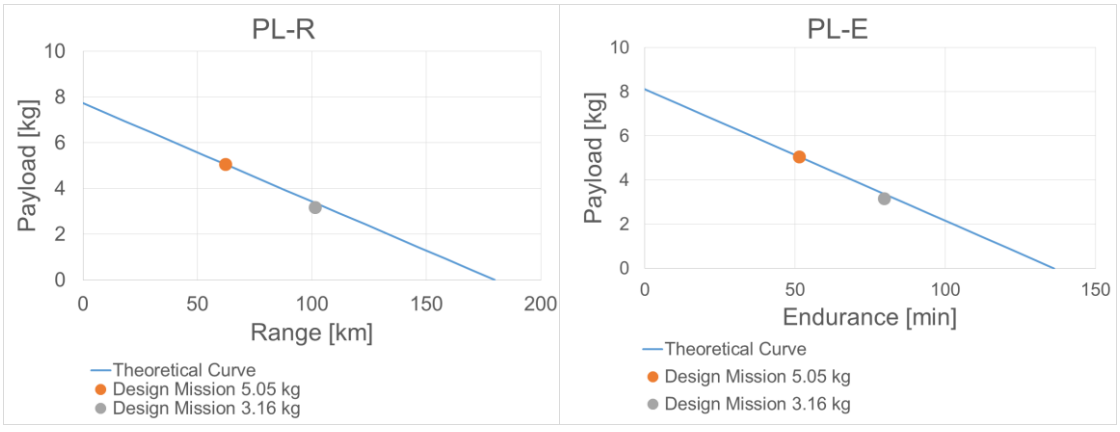

Figure 3-2 Theoretical Payload-Range curve (left) and theoretical Payload-Endurance curve (right).

	Units	Value
Rear Motor	-	AXI 5330/18
Rear Propeller	-	APC 19x12
Cruise speed	m/s	42
Maximum Ascent Angle (MAA)	º	9.5
Vertical speed for MAA	m/s	5.11
PL	kg	5.79
Batteries Weight	kg	3.06
Batteries Voltage	V	37
Batteries Capacity	Ah	15
Cruise Endurance	min	9.4
Range	km	24.7

Table 3-2 Alternative configuration and performance.

It is important to remark that all obtained results related to the performance of the aircraft have been calculated making use of the tables of performance data from APC Propellers and AXI motors with the program e-calc. The curves provided by this program have been checked with the data of the manufacturer to ensure the accuracy of the results. After that, the process followed to obtain every cruising operating point has consisted on calculating the curve of required power to move the propeller at the shaft motor station and the curve that results of the intersection of the required power to flight (calculated with aerodynamics) and the available power after the propeller (calculated with propulsion plant). Thus, the model takes into account the battery, the motor and the propeller efficiencies, as well as the complete polar of the aircraft and the flight level. The battery efficiency has been considered constant, although it depends on the temperature. The motor efficiency and its angular rate depend on the feed current. Finally, propeller efficiency depends on the flying speed and the angular rate, in the way APC says.

3.3. WIND CONDITIONS

The capability of sustained flight while the RPA experiences 10 m/s head and cross wind is a requisite of the design mission. A study has been conducted in order to check the rudder deflection that satisfies this requirement. The result of this study highlights that a deflection of 7.78 degrees of each rudder is sufficient to maintain null the yawing moment due to this cross wind at the design mission conditions. The ratio between horizontal speed and cross wind for the design mission results in an Angle of Sideslip (AoS, β) of 23.4º. The head wind only affects the aerodynamic velocity, and so this affects the range that the aircraft can achieve. In the case of wind blowing from the rear, the range increases to 69.8 km for 5.05 kg of PL or to 113.9 km for 3.16 kg of PL. On the other hand, if wind blows from the front, the range decreases to 54.8 km for 5.05 kg of PL or to 89.4 km for 3.16 kg of PL.

In Figure 3-3 the maximum borne gust intensity is shown on the left hand side. When the aircraft experiences a gust, the vertical speed that the wings experiences is different than that of cruise flight. This vertical speed induces an Angle of Attack (AoA) and an increment of loading to the wings. The blue line is the maximum gust intensity that satisfies the load factor of 3.8 established by regulations. The horizontal green line is the gust intensity that induces stall AoA in the front wing. For this last calculation, a simple model considering that all wing is experiencing the same vertical gust speed has been used. On the right hand side of the same figure, the required rudder deflection to cancel the yawing moment in presence of cross wind is illustrated. In this case, as there are two

rudder controls, the same deflection of both control-surfaces has been supposed in calculating the needed deflection.

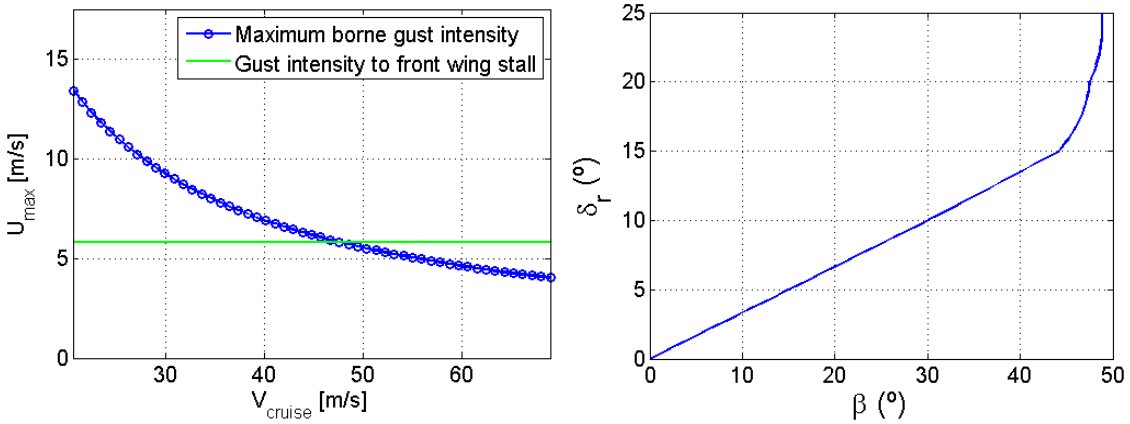

Figure 3-3 Maximum borne gust intensity with cruise speed (left) and rudder deflection with sideslip angle to cancel yawing moment.

3.4. FLIGHT ENVELOPE

The flight envelope obtained is based on military regulation (NATO, 2007) because there is no civil normative applicable to this aircraft which specifies constraints to the flight envelope. Figure 3-4 shows the results based on direct application of this regulation for manoeuvre envelope without and with flaps, and also gusts envelope. These two graphs indicate boundaries which the aircraft should not cross during flight and also the structure must bear all the loads transmitted to the aircraft at whichever point of the diagrams.

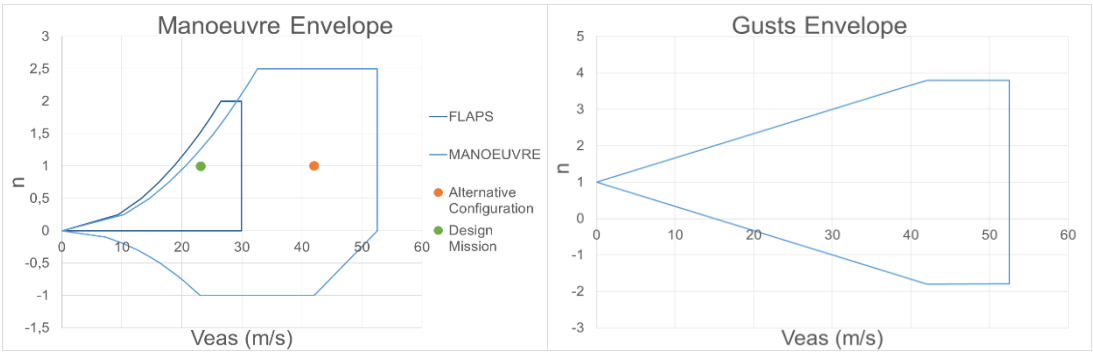

Figure 3-4 Manoeuvre Envelope (left) and Gusts Envelope (right).

3.5. LAUNCHING AND RECOVERY PERFORMANCES

3.5.1. Landing as fixed wing

The objective of this section is to analyze the vertical speed in order to estimate the main landing gear behaviour. The first step is to calculate the stall speed, then the landing speed in clean configuration and with the flaps deflected. Then the angle of attack can be determined, and supposing a reasonable descent angle, the vertical speed of the aircraft can be obtained as:

$$\dot{ho} = V \sin \Upsilon = \begin{cases} 1.4\ m/s \\ 0.41\ m/s \end{cases}$$

It is possible to make a dynamic model of the landing gear in the form:

$$\ddot{M}h + F\,\dot{h} + Kh = (0.45 * W + \dot{ho})\delta(t)$$

Therefore, the expression can be rewritten as:

$$\ddot{h} + 2\varsigma\omega n\,\dot{h} + \omega n^2 h = 0$$

$$\dot{h}(0) = \frac{(0.45 * W + \dot{ho})}{M}$$

$$h(0) = 0$$

	Units	Value
E	GPa	70
I	Kg·m^2	0.0404
L	m	0.696
K	N/m	2.545E10
M	kg	0.25

Table 3-3 Properties of the landing gear.

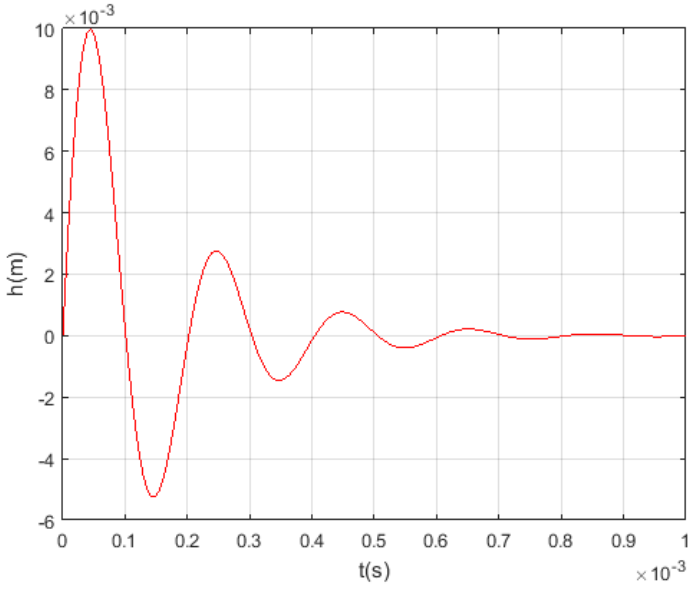

Figure 3-5 Dynamic Response.

The kinetic energy at the moment of the touchdown can be dissipated in a few millimeters, which compared to the length of the bars is acceptable.

3.5.2. Parachute performances

Parachute system should be used in situations involving loss of control of the vehicle, when the high kinetic energy of the impact could be a serious danger for the payload, the vehicle or the land property. These are some situations which could lead to a deployment:

- Communication lost/control lost.
- Bird strike, structural damage…
- Spin/stall recovery.
- Power loss after takeoff/before landing.

In the first and second cases a deployment during cruise phase would be needed. The limiting factor during a high speed deployment is the opening force of the chute. Although

the Kevlar® braces would possibly resist up to 10^4 N, the material of the chute or even the airframe could be damaged. After a high speed deployment, the vehicle would immediately stall, causing an oscillatory effect during steady descent, hard to control with the chute.

It would be desirable to perform or program a controlled stall or a steady flight over a safe zone before deployment.

During a stall or the takeoff/landing stage, the horizontal speed would be minimum, so the opening force and the oscillation are considerably reduced. However, the limiting factor is the deployment height. After a zero speed deployment, there will be a height loss during the time needed to extent braces and fill the canopy, to achieve an effective deceleration. The deployment time of the Skycat® XL96 system is approximately 2.8 s for a zero speed deployment, decreasing as vertical speed increases. So, the time from failure detection to deployment if the vehicle is in freefall, should be minimized. The ideal condition is a deployment at zero vertical speed, where the safe minimum deployment height (distance to reach terminal speed) would be around 30 m. Below this height, the parachute would not completely fill and the impact speed would be higher.

As the vertical speed rises, the minimum height increases too, because even if the filling time is lower, the distance would be higher.

The opening force has been calculated by the canopy load method (Figure 3-6 left). Below the stall speed, the forces will mainly be due to the vertical speed reached on freefall during opening process. The minimum height (Figure 3-6 right) has been calculated through simplifying assumptions and the result for zero vertical speed approximates the more optimistic manufacturer specification (25 m).

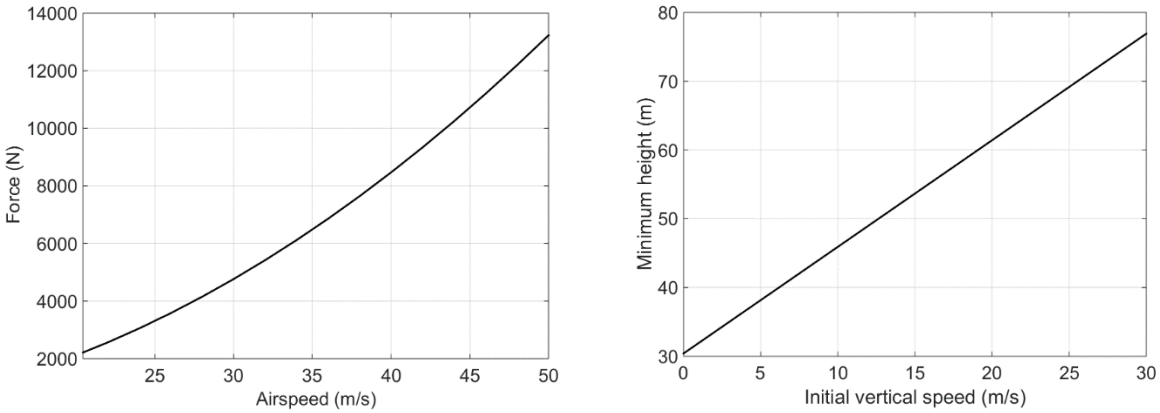

Figure 3-6 Parachute opening forces (left) and minimum safe deployment height (right).

3.6. LANDING PLATFORM

The specifications of the challenge require that the payload be accessible from the lower side of the aircraft. While the aircraft has been designed to allow this to be done manually, it is desirable to have a system that brings the payload in a more accessible way to the human operator. This system should be relatively light and compact to facilitate its transportation and implementation, and is the landing platform presented in this page.

A special access point would be available to place the payload for loading, or to retrieve it for unloading. A moving arm would shift the load from the access point to the payload bay and vice versa. For more information on the payload integration turn to Section 2.4.

The induction charging system described in Section 2.3**¡Error! No se encuentra el origen de la referencia.** could be incorporated to this system as a module, since battery charging is done when the aircraft is at rest on the landing platform.

Some missions may require a broader range than that which the RPA itself can provide. In these cases, platforms could be installed along the planned route so that the aircraft may recharge its batteries and continue with its mission afterwards. These intermediate charging platforms could be placed anywhere, from the top of buildings in an urban area to the decks of ships in the sea. The main induction module should be designed to take the mains voltage input. If these platforms are to be placed outside an urban area, they could take the energy from transmission towers. In this case, an additional module reducing the high voltage would need to be included.

It is clear that high precision landing is needed, because both the moving arm and the coils must be perfectly aligned to ensure a correct functioning. To this purpose, three different alignment systems are described:

- Computer vision: The electro-optical camera of the RPA could detect a pattern on the platform.
- Electromagnetic sensor: The intensity of the electromagnetic field generated by the induction charging system is measured inside the RPA, and corrective measures are taken to ensure a proper alignment.
- Ultrasonic detectors: During the last stages of the landing process, ultrasonic detectors could be used to measure the position of the RPA relative to the platform.

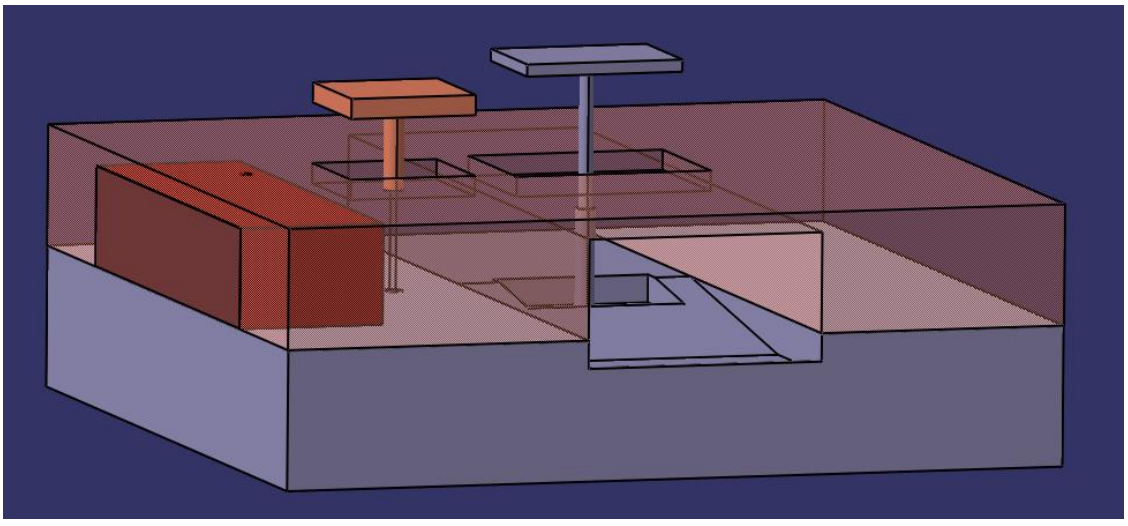

Figure 3-7 Representation of the three-module landing platform.

3.7. MODULARITY AND HANDLING

Nowadays modularity is a crucial aspect for designers and operators. This feature allows the product to be easily handled and provides versatility in order to adapt it to new possible scenarios.

This aircraft concept has been developed taking into account modularity. Thus, the structure is divided in different individual elements:

- Fuselage: The overall length of this element is 1.99 m in order to satisfy the requirements of transportability. In addition, the rear-end can be disassembled to change the rear propulsion system. The internal structure has been designed keeping in mind that the equipment would be different depending on the mission. Because of this, the localization of the equipment inside the fuselage is variable. In spite of this, the final disposition must provide a high enough static margin.
- Wings: The two wings are divided in two parts. Each part corresponds to a half-wing as it has been explained in Section 2.2. The dimensions of the half-wings are compatible with the transportability requirements. Other different wings can be assembled to perform alternative missions.
- VTOL motor-housing: These parts can be easily removed to change these motors, or if hover flight and VTOL were not required.
- Landing gear: The landing gear is easily demounted from the fuselage in the case that an alternative system was desirable.
- Payload: The payload compartment has been designed to accommodate a container inside of which the desired payload is placed. This capability allows to change the payload ensuring the complete integration inside the fuselage. Besides, the door of this compartment is interchangeable in order to allow the payload functioning, for instance a camera that needs to be partly out of the fuselage. The payload system has the possibility to deliver the payload during flight if mission requires it.
- Swappable batteries: The batteries used can be easily interchanged. This feature provides the capability of reducing the time spent by the aircraft on ground between missions. This is very interesting in missions where persistence is important because of the reduction of the number of required aircraft.

In conclusion, the modularity design makes this aircraft a multirole platform and perfect to accomplish whatever mission no matter how different they are.

3.8. MAINTENANCE

This section is divided in two different parts: one for the RPA and another for the landing platform.

The aircraft design has been thought to minimize costs and maintenance. So, all parts are easily accessible in order to replace components in a rapid and cheaper way. The proposed required maintenance consists in three different tasks:

1. *Daily maintenance.* The following procedure must be conducted before and after every flight.
    - Visual check of the propellers.
    - Manual check of the propeller attachment and its fasteners.
    - Manual check of the free turn of the motors.
    - Manual check of the motor shaft fastening.
    - Check the battery connectors.
    - Check the voltage of every battery.
    - Manual and visual check of the landing gear and its attachment.
    - Check the wiring.

- Manual and visual check of the antennas health.
- Check the behaviour of the antennas and GPS.
- Check the behaviour of the aircraft when moving the controls.

2. *Service maintenance: weekly or every 25 flight hours.*
    - Visual exhaustive inspection of the fuselage, landing gear, and other structural components in order to detect cracks and other damages.
    - Verify the fasteners of all structure and attached parts.
    - Clean and check the battery connectors.
    - Check the calibration of the compass.
    - Check the health of the batteries.
3. *Basic and general maintenance: monthly or every 100 flight hours.*
    - Exhaustive inspection of the propellers and substitution if necessary.
    - Exhaustive inspection of the structure.
    - Exhaustive inspection of the landing gear and its attachment.
    - Exhaustive inspection of wiring and connectors.
    - Exhaustive inspection and cleaning of electronic boards.
    - Exhaustive inspection of fasteners.
    - Check working voltage of electronic components.
    - Check the behaviour of each controller.
    - Verify IMU calibration.
    - Inspection, and substitution if required, of the bearings of all motors.
    - Check if there are software updates available.

The landing platform follows industrial regulations and thus it is not going to be described in detail.

3.9. OTHER MISSIONS

In addition to the principal mission for which the RPA was designed, it will be able to perform other transport missions at greater distance, provided that there are enough induction recharging platforms (Section 2.3) along the trajectory.

On the other hand, the RPA will be able to perform other missions which are mentioned later. The payload requirement in most cases is an electro-optical camera, which is incorporated in the RPA, an infrared camera or a special sensor. In this case, it will be able to use the rest of the weight that was initially used as payload, to increase the number of batteries and therefore rise range and endurance (Table 3-4).

Table 3-4 shows some other possible missions (Austin, 2010), persistent hours required and payload requirements, among others.

Mission	Required persistence hours	Number of RPAs	Set of batteries	Payload requirements
Cargo mission	-/-	1	1	-/-
Crop monitoring	-/-	1	1	IR camera
Monitoring for pollution	-/-	1	1	Special sensor
Meteorological sampling	-/-	1	1	Special sensor
Survey tasks	-/-	1	1	EO survey camera
Monitoring of traffic in sea-lanes, coastlines for debris or rescue operation	12	2	2	IR camera
Traffic monitoring	12	2	2	-/-
Monitoring watercourse flow and water levels	12	2	2	-/-
Surveillance of coastline, ports, bridges and other access points for the import of illegal substances	24	3	4	IR camera
Support in emergency situation	24	3	4	-/-
Inspection of power-lines	24	3	4	IR camera
Fire prevention and monitoring	24	3	4	IR camera
Inspection of gas and oil supplies	24	3	4	IR camera

Table 3-4 Different possible missions.

The estimated values for specifications of the different payload configurations are:

- Without extra payload: Range: 170 Km; Endurance: 130 min
- Infrared camera: Range: 135 Km; Endurance: 100 min
- EO survey camera: Range: 110 Km; Endurance: 90 min

3.10. SAFETY

Risk analysis aims to facilitate the identification and resolution of problems that may arise during the RPAS operation.

In order to conduct this study, a preliminary list of hazards has been elaborated, in which risks have been evaluated according to their frequency, severity and risk level. In addition, some potential solutions have been proposed for each case, which result in a certain value of residual risk level.

Each risk has been evaluated with the MIL-STD-882D / E normative criteria (MIL-STD-882E, 2012), which has been presented in the following tables:

Description	Level	Specific individual item
Frequent	A	Likely to occur often in the life of an item.
Probable	B	Will occur several times in the life of an item
Occasional	C	Likely to occur sometime in the life of an item.
Remote	D	Unlikely, but possible to occur in the life of an ítem.
Improbable	E	So unlikely, it can be assumed occurrence may not be experienced in the life of an item.
Eliminated	F	Incapable of occurence. This level is used when potential hazards are identified and later eliminated.

Table 3-5 Probability levels.

Description	Severity category	Mishap Result Criteria
Catastrophic	1	Could result in one or more of the following: death, permanent total disability, irreversible significant environmental impact, or monetary loss equal to or exceeding $10M.
Critical	2	Could result in one or more of the following: permanent partial disability, injuries or occupational illness that may result in hospitalization of at least three personnel, reversible significant environmental impact, or monetary loss equal to or exceeding $1M but less than $10M.
Marginal	3	Could result in one or more of the following: injury or occupational illness resulting in one or more lost work day(s), reversible moderate environmental impact, or monetary loss equal to or exceeding $100K but less than $1M.
Negligible	4	Could result in one or more of the following: injury or occupational illness not resulting in a lost work day, minimal environmental impact, or monetary loss less than $100K.

Table 3-6 Severity categories.

The risk value has been established with the following table:

	Catastrophic	Critical	Marginal	Negligible
Frequent	1	3	7	13
Probable	2	5	9	16
Occasional	4	6	11	18
Remote	8	10	14	19
Improbable	12	15	17	20

Table 3-7 Risk value.

Risk matrix:

SEVERITY / PROBABILITY	Catastrophic (1)	Critical (2)	Marginal (3)	Negligible (4)
Frequent (A)	High	High	Serious	Medium
Probable (B)	High	High	Serious	Medium
Occasional (C)	High	Serious	Medium	Low
Remote (D)	Serious	Medium	Medium	Low
Improbable (E)	Medium	Medium	Medium	Low
Eliminated (F)	Eliminated			

Figure 3-8 Risk matrix.

3.10.1. Risks analysis

The following table presents an analysis of general risks and the possible solutions which could mitigate these hazards:

EXTERNAL ELEMENTS						
HAZARD DESIGNATION	POTLUCK	SEVERITY	RISK LEVEL	RISK VALUE	POTENTIAL SOLUTIONS	RESIDUAL RISK LEVEL
Rainfall	A	Negligible	Medium	13	Meteo check, NO-GO	Low
Hail	B	Catastrophic	High	2	Meteo check, NO-GO	High
Bird impact	A	Marginal	Serious	7	Damage evaluation, Parachute	Serious
Proximity to other RPAS	D	Critical	Medium	10	Operation in segregated airspace	Medium
High voltage lines	B	Critical	High	5	Mission route planning	Medium
Track condition	C	Critical	Serious	6	Track check, quadcopter mode	Low

Table 3-8 Risk analysis of external elements.

RPAS SYSTEMS						
HAZARD DESIGNATION	POTLUCK	SEVERITY	RISK LEVEL	RISK VALUE	POTENTIAL SOLUTIONS	RESIDUAL RISK LEVEL
Propulsion system failure	C	Catastrophic	High	4	Revision, maintenance	Critical
Rotor failure	C	Catastrophic	High	4	Revision, maintenance, fixed wing mode, parachute	Medium
Battery failure	C	Catastrophic	High	4	Revision, charge condition, maintenance	High
Battery exhaustion	E	Catastrophic	Medium	8	Route planning	Medium
Camera failure	C	Marginal	Medium	11	Maintenance	Medium
Landing/TO platform failure	C	Marginal	Medium	11	Maintenance, replacement unit, manual control	Low
Light system failure	D	Marginal	Medium	14	Operator guidance, camera, exterior lights	Medium

Table 3-9 Risk analysis of RPAS systems.

COMMUNICATIONS AND DATA LINK						
HAZARD DESIGNATION	POTLUCK	SEVERITY	RISK LEVEL	RISK VALUE	POTENTIAL SOLUTIONS	RESIDUAL RISK LEVEL
Hack	D	Catastrophic	Serious	8	Encrypt code	Serious
Ground control station loss	E	Marginal	Medium	17	Back Home, parachute	Low
GPS failure	D	Marginal	Medium	14	Manual control, pre-check GPS	Medium
Interferences: electromagnetic, radio waves	D	Critical	Serious	10	Route check, avoidance of possible hazards	Medium

Table 3-10 Risk analysis of communications and data link.

RPAS CELL						
HAZARD DESIGNATION	POTLUCK	SEVERITY	RISK LEVEL	RISK VALUE	POTENTIAL SOLUTIONS	RESIDUAL RISK LEVEL
Hull damage	E	Critical	Medium	15	Revision, maintenance	Low
Structural component loss	E	Catastrophic	Medium	12	Revision, maintenance	Low
Fire/explosion	E	Catastrophic	Medium	12	Revision, maintenance	Low
Collision	D	Catastrophic	Serious	8	Parachute	Serious
Payload loss	E	Catastrophic	Medium	12	Revision, check	Low
Hull damage	E	Critical	Medium	15	Revision, maintenance	Low

Table 3-11 Risk analysis of RPAS cell.

FLIGHT CONDITIONS AND OPERATOR						
HAZARD DESIGNATION	**POTLUCK**	**SEVERITY**	**RISK LEVEL**	**RISK VALUE**	**POTENTIAL SOLUTIONS**	**RESIDUAL RISK LEVEL**
Wrong command interpretation	E	Critical	Medium	15	Route planning	Low
Wrong manoeuvre by the operator	D	Marginal	Medium	14	Operator training	Low
Loss of control	D	Critical	Medium	10	Operator training	Medium
Wrong mission planning	E	Negligible	Low	20	Mission check	Low
Wrong input of flight parameters	E	Marginal	Medium	17	PRE-FLIGHT Check	Low
Stall	D	Critical	Medium	10	CL MAX, V STALL (Autopilot), parachute	Low

Table 3-12 Risk analysis of flight conditions and operator.

3.10.2. Safety assessment of the design mission

The Safety Assessment analyses the hazards and risks that are applicable to the different phases of the design mission. Most of the hazards listed above could apply to any mission segment: Take-off, cruise, 5 minute loiter and landing. In this case, the potential solutions proposed in the table could be applied in any of the phases.

However, should a dangerous situation be more probable or have a higher severity in a certain phase of the mission, it will be analysed separately. Moreover, the risk could be solved in a particular way depending on the phase of the mission, so the following solutions are more specific of the mission phase in which the RPAS is operating.

1a) Take-off (vertical)

- Landing/TO platform failure: possibility of fixed-wing Take-off should an adequate runway be available.
- Rotor failure: parachute.
- Propulsion system failure: parachute.

1b) Take-off (fixed-wing mode)

- Inadequate track condition: vertical Take-off if a platform is available.
- Propulsion system failure: abort Take-off if possible, parachute.

2) Cruise

- Propulsion system failure, battery failure: land in nearest available safe zone deploying the parachute.
- Battery exhaustion: mission planning, land in nearest recharge platform in a high voltage line tower equipped with one. Should it not be possible, land in nearest available safe zone deploying the parachute.

- Ground control station loss: mission planning, autopilot back home protocol to recover communication. Should it not be possible, land in nearest available safe zone deploying the parachute.
- Loss of control, stall: operator training, autopilot.

3) Loiter (5 minute)

- Propulsion system failure, battery failure: land in nearest available safe zone deploying the parachute.
- Battery exhaustion: mission planning, land in nearest recharge platform in a high voltage line tower equipped with one. Should it not be possible, land in nearest available safe zone deploying the parachute.
- Ground control station loss: mission planning, autopilot back home protocol to recover communication. Should it not be possible, land in nearest available safe zone deploying the parachute.
- Loss of control, stall: operator training, autopilot.

4a) Landing (vertical)

- Camera failure: GPS, automatic landing procedure (autopilot).
- Landing/TO platform failure: possibility of fixed-wing landing should an adequate runway be available.
- Light system failure: guidance by operator on landing zone, exterior lights, camera.

4b) Landing (fixed-wing mode)

- Inadequate track condition: vertical landing if a platform is available.
- Light system failure: guidance by operator on landing zone, exterior lights, camera.
- Camera failure: GPS, automatic landing procedure (autopilot).

3.11. COSTS

In this chapter a simple cost model is presented. In the sector of RPAS, it is difficult to find an accurate description in terms of how to calculate costs for small RPAS, as most of them are military programs. These types of programs are at the cutting edge of technology which makes the provided information less trustable, as it is top secret. The expressions used in this chapter are mainly from civil aviation so, presumably, there will be significant differences regarding a real situation. Nevertheless, it is important to have a first approximation in mind and, to understand it, as a start point.

3.11.1. Total investment

At first the total investment has been calculated. It has been divided into four main groups: structure, powerplant (electric motors, propellers and speed controllers), batteries and payload (cameras, parachute, sensors, equipment…).

The price of the structure, in US$, is defined by:

$$PC = 3370 \cdot (Airframe\ weight)^{0.9}$$

With the airframe weight in kg, therefore:

$$PC = 30.238\$$$

The second group has: 5 electric motors, plus their respective speed controller and propellers. This prices can be obtained directly from the manufacturer.

$$PM = 5 \cdot EM + 5 \cdot P + 5 \cdot ESC$$

Where EM corresponds to the price of the electrical motor, in this case, the AXI 5320/28 Gold Line V2, P is the price of the propeller APC 17x8 E and, the ESC is price of the speed controller Jet Spin 75 OPTO.

$$PM = 2.185\$$$

For the battery group, depending on the type of mission, the price will vary, because different batteries are used, so:

$$PB_{60km} = 569.97\$$$

$$PB_{100km} = 1269.97\$$$

In terms of equipment, depending on different manufacturers, capacities and qualities there is a wide variety of prices available. Based on a high quality market, as there are no limitations in costs, a price for the equipment of 9.300$ has been considered.

Finally, the total investment is defined by:

$$TI = 1.1 \cdot PC + 1.3 \cdot PM + 1.3 \cdot PB$$

In each case:

$$TI_{60km} = 46.185\$$$

$$TI_{100km} = 47.095\$$$

3.11.2. Direct Operating Cost (DOC)

Direct operating costs for the RPA are ideally presented and they should only be understood as a starting point for the DOC process analysis. Based on the assumption that the RPA will be operating 24h a day during one year, the RPA will be flying during 2179h and will be charging, around 2503h for the 60km mission whereas for the 100km mission this relation is 1820/1613h, respectively. T_{block} or block time is defined as the sum of the mission time and the charging time, 1,87h and 2,33h for 60 and 100km missions respectively. One hour charging has been assumed for both missions.

The DOC is usually defined as the sum of:

DOCflt	Ccrew, Celectricity
DOCmaint	Maintenance costs
DOCdev	Devaluation of components
DOCins	Cost of insurances

Table 3-13 DOC breakdown.

The expressions used for the calculation of these four groups are given in Roskam, 1990. The DOCflt the cost of electricity is based on the price of a kWh in Spain, 0.15€/kWh. The DOCmaint represents the highest % of the DOC even though small UAVs are less expensive; there are a lot of small elements that can be damaged during normal operation as propellers. Batteries are the components that suffer more throughout the life of the RPA. A life of 350 cycles (charge-discharge) per battery has been assumed, which annually means a total of 14 battery packs for the 60km mission and 11 for the 100km mission. On the other hand, brushless motors used in a healthy way could last longer than a year; therefore, assuming a change of all the main powerplant components each year is a good point in between. The devaluation of component is really low and the insurances have been assumed of a 2% of the total DOC.

The following two tables represent the DOC for 60km and for 100km:

DOC (60km)	
$/nm	1,8
$/km	1,0
€/km	0,9
€/mission	52,5
€/day	167,6
€/month	5026,8
M€/yr	1,8

DOC (100km)	
$/nm	2,2
$/km	1,2
€/km	1,1
€/mission	105,9
€/day	267,2
€/month	8016,9
M€/yr	2,9

Table 3-14 DOC for both missions.

As it can be seen in the results, the return of investment (ROI) is guaranteed. There are several reasons to support this, like a presumable reduction of the insurance premium for a third party as well as for damages of infrastructures. As a basis of risk management: fewer risks, less premiums. Besides, the social benefit and the improvements in security will be significantly reinforced. As a matter of fact many companies are using UAVs with different purposes, not only Facebook or Amazon but also top insurance companies in industrial risk management such as, AIG, Allstate, etc.

The following figure shows a mid-term projected sales of UAVs only in the United States given in (Association for Unmanned Vehicle Systems International, 2013).

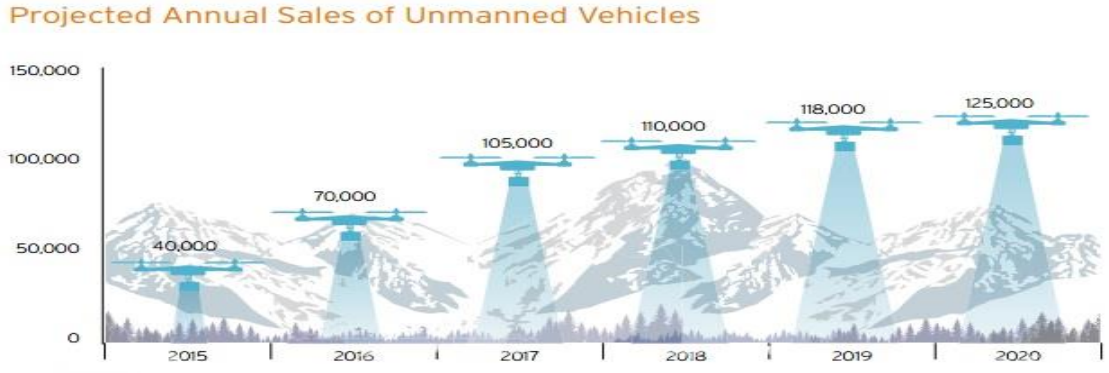

Figure 3-9 Projected Annual Sales of UAVs in USA.

In conclusion, it can be can be said that this chapter is only the prelude to a deeper cost analysis really interesting, which, even nowadays (mid 2016) have different paths to be followed. There are many assumptions made without a really knowledge of what RPAS companies do in real life. Besides that, it is considered a good start point for the introduction of small RPAS in the world of economics.

4. FUTURE

In the recent years, the investment in the sector of RPAS has increased substantially. Furthermore, the number of civil missions which these aircraft can achieve is in continuous growth. However, there is still much effort to be done in order to integrate these aircraft in the non-segregated airspace, which include the development of new regulations and technologies. In any case, their incorporation in the non-segregated airspace is progressively being accomplished.

Additionally, the importance of emissions in aviation is a fact to be taken into account, thus great efforts are being made to reduce the pollution and noise of these aircraft, especially near urban zones (NASA, 2013). The future perspective is that of a continuous reduction in these emissions, where electric power-plants are becoming a fundamental part of the solution.

As can be seen, this RPA is a very suitable solution to accommodate all these tendencies unified into a single product. From the viewpoint of green aviation, it takes the previously mentioned objectives a step further, as the electric power-plant proves very advantageous regarding both objectives of green aviation: eliminating pollution and reducing noise. Also, from the standpoint of developing new technologies, it can also prove valuable as a low-cost platform for testing a wide variety new equipment, which is possible in great part due to its modularity. Another advantage of the modularity of this aircraft is the possibility to modify any of the modular components as required, which can accommodate the aircraft to different types of missions.

That also means that the aircraft can be rescaled into bigger platforms adapting the platform to different regulatory weight categories. The design of this RPA has taken into account the normative so that in the rescaling process it would be possible to achieve what the regulation establishes.

One of the possible future designs for this aircraft could be enlarging the fuselage introducing fuselage sections both before and after the centre of gravity, maintaining a desired stability. The landing gear could also be adapted to the new aircraft weight. In addition, the wing could not only be rescaled but also it could be modified into other configurations, for instance: conventional configuration, canard, joined wing, etc. In order to provide enough thrust to the new versions of the RPA, changing the propulsion system for a larger one would be necessary. For example, an AF-130 electric motor provides enough power to operate aircraft of weights up to 500 kg (EVO Electric Ltd., 2011).

In conclusion, this RPA fits perfectly into all these trends of technological evolution, while maintaining low design and operational costs. Besides, the possibility to design, develop and manufacture new modular components and innovative equipment make the Libis the ideal platform to accomplish both current and future applications in the sector of RPAS.

REFERENCES

Angrisani, L., d'Alessandro, G., D'Arco, M., Paciello, V. and Pietrosanto, A., "Autonomous recharge of RPAs through an induction based power transfer system," *Measurements & Networking (M&N), 2015 IEEE International Workshop on*, Coimbra, 2015, pp. 1-6. doi: 10.1109/IWMN.2015.7322968.

Association for Unmanned Vehicle Systems International, *"The Economic Impact of Unmanned Aircraft Systems Integration in the United States,"* Arlington, USA, March, 2013.

Austin, Reg, 2010. Unmanned aircraft systems: UAVS design, development and deployment. John Wiley & Son, Ltd.

Else (CEO), A., 2016. MaxAmps. Available at: http://www.maxamps.com/.

EVO Electric Ltd., *"AF-130 Motor | Generator AF-130 Specification Performance and Efficiency (Motor Operation),"* vol. 44, no. 0. EVO Electric Ltd., pp. 1–2, 2011.

Knacke, T. W., 1991. *Parachute Recovery Systems Design Manual* 1st edit. For Publishing, Santa Barbara.

MIL-STD-882E, 2012. *Mil-Std-882D Standard Practice for System Safety.*

National Aeronautics and Space Administration (NASA), *"Green Aviation: A Better Way to Treat the Planet."* NASA Facts, Washington, pp. 1–2, 2013.

Roskam, J., 1973. Methods For Estimating Stability And Control Derivatives Of Conventional Subsonic Airplanes Second edi., Lawrence, Kansas.

Roskam, J., 1987. *Airplane Design: Part VI* First edit. R. A. and E. Corporation, ed., Lawrence, Kansas.

Roskam, J., 1990. *"Airplane Design Part VIII: Airplane Cost Estimation: Design, Development, Manufacturing and Operating,"* Kansas.

Torenbeek, E., 1976. *Synthesis of subsonic airplane design* D. U. Press, ed., Delft.

A. ANNEX. STABILITY DERIVATIVES

The stability derivatives presented in Table A-1 have been calculated by different methods. Despite Tornado has been used to calculate some aerodynamic results, it has not been used to calculate the stability derivatives because Tornado does not take into account the fuselage. Roskam's procedure is very similar to DATCOM, however there are differences in the coefficients related to roll and yawing rate. In addition, DATCOM only admits NACA aerodynamic profiles, and Libis has a Clark-Y B profile. Due to this, the relative error between Roskam and DATCOM in certain longitudinal moment, rolling and yawing derivatives is higher (Torenbeek, 1976; Roskam, 1987 & Roskam, 1973).

			ROSKAM & TORENBEEK	AVL	DATCOM	AVL RELATIVE ERROR	DATCOM RELATIVE ERROR
LONGITUDINAL STABILITY	0	C_{D0}	0.024	-	0.023	-	-4.79%
		C_{L0}	0.181	0.155	0.177	16.83%	-2.31%
		C_{m0}	-0.003	0.0114	-0.052	-76.30%	94.80%
	α	$C_{D\alpha}$	0.239	-		-	-
		$C_{L\alpha}$	4.138	4.038	4.245	2.48%	2.52%
		$C_{m\alpha}$	-0.707	-0.593	-0.944	19.21%	25.13%
	$\dot{\alpha}$	$C_{D\dot{\alpha}}$	0.000	-	-	-	-
		$C_{L\dot{\alpha}}$	7.411	-	-	-	-
		$C_{m\dot{\alpha}}$	-4.063	-	-	-	-
	q	C_{Dq}	0.000	-	-	-	-
		C_{Lq}	6.248	12.92	6.35	-51.64%	1.61%
		C_{mq}	-18.410	-27.78	-19.24	-33.73%	4.32%
	δ_e	$C_{D\delta e}$	0.005	-	-	-	-
		$C_{L\delta e}$	1.391	-	-	-	-
		$C_{m\delta e}$	-2.930	-	-	-	-
LATERAL-DIRECTIONAL STABILITY	β	$C_{Y\beta}$	-0.425	-0.395	-0.392	7.60%	-8.48%
		$C_{l\beta}$	-0.0286	-0.009	-0.0303	204.61%	5.53%
		$C_{n\beta}$	0.0170	0.025	0.0176	-31.91%	3.28%
	p	C_{Yp}	-0.004	0.0003	-0.00057	1208.69%	-586.38%
		C_{lp}	-0.472	-0.39	-0.493	21.14%	4.07%
		C_{np}	-0.019	-0.005	-0.006	271.75%	-199.80%
	r	C_{Yr}	0.120	0.28	-	-57.15%	-
		C_{lr}	0.049	0.027	0.032	82.22%	-52.04%
		C_{nr}	-0.040	-0.093	-0.052	-57.12%	23.32%
	δ_A	$C_{Y\delta A}$	0.000	-		-	-
		$C_{l\delta A}$	0.250	-		-	-
		$C_{n\delta A}$	-0.002	-		-	-
	δ_r	$C_{Y\delta r}$	-0.212	-		-	-
		$C_{l\delta r}$	-0.002	-		-	-
		$C_{n\delta r}$	0.051	-		-	-

Table A-1 Stability derivatives from different methods.

B. ANNEX. DRAWINGS

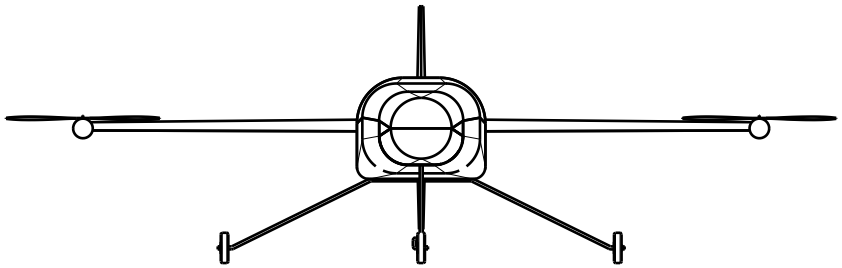

Libis

DRAWING TITLE: Front View

DRAWN BY: XXX	DATE: 19/05/2016	SIZE: A4	DRAWING NUMBER: XXX	REV: X
CHECKED BY: XXX	DATE: XXX			
DESIGNED BY: XXX	DATE: XXX	SCALE 1:25	WEIGHT(kg) 25	SHEET 1/3

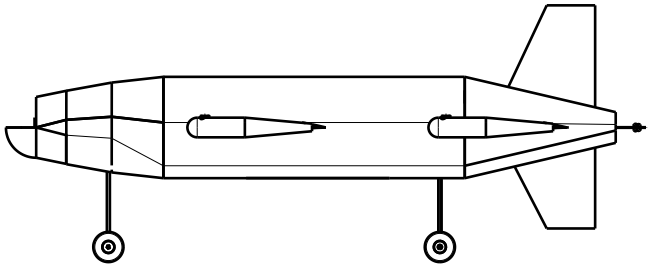

Libis

DRAWING TITLE: Side View

DRAWN BY	DATE
XXX	19/05/2016
CHECKED BY	DATE
XXX	XXX
DESIGNED BY	DATE
XXX	XXX

SIZE	DRAWING NUMBER	REV
A4	XXX	X

SCALE	WEIGHT(kg)		SHEET
1:25	25		2/3

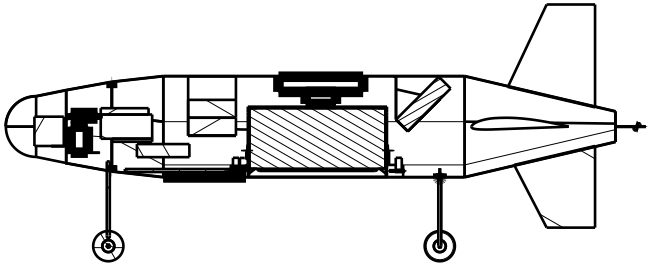

Section view A-A

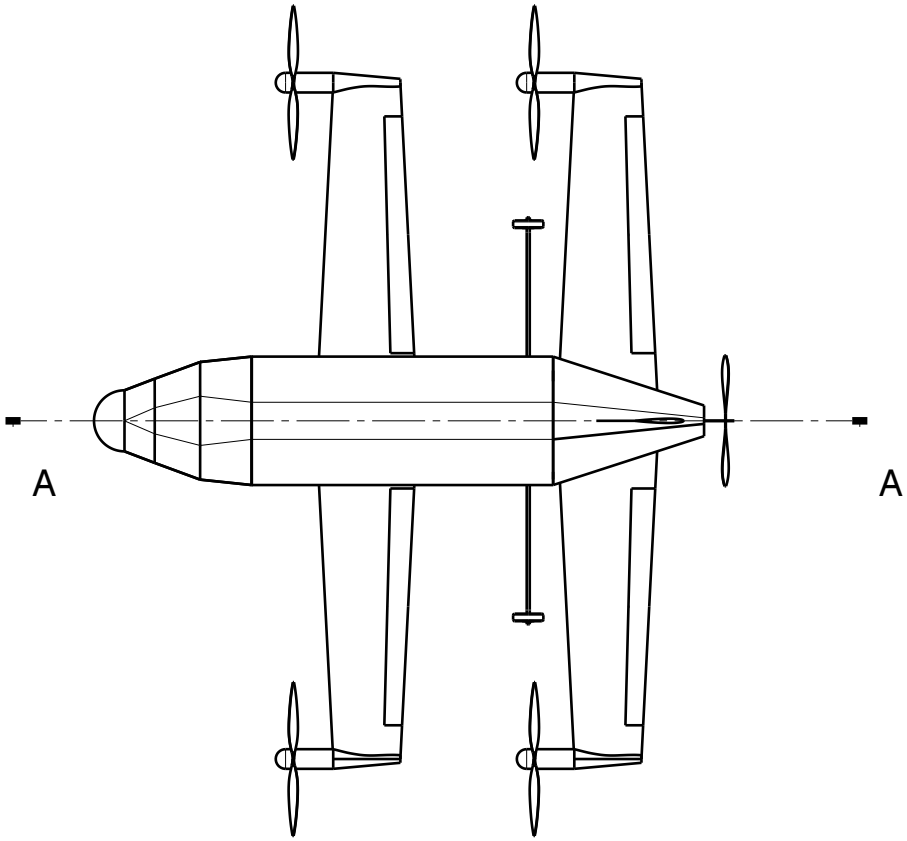

DRAWN BY XXX	DATE 19/05/2016	Libis			
		DRAWING TITLE Top View			
CHECKED BY XXX	DATE XXX	SIZE A4	DRAWING NUMBER XXX		REV X
DESIGNED BY XXX	DATE XXX	SCALE 1:25	WEIGHT(kg) 25		SHEET 3/3